Large-Scale Structure Evolution in Axisymmetric, Compressible Free-Shear Layers

by

D.P. Aeschliman and R.S. Baty

Aerosciences & Compressible Fluid Mechanics Department
Sandia National Laboratories (SAN)
Albuquerque, NM USA

Presented at the 87th Semi-Annual Meeting of the
Supersonic Tunnel Association, International
May 4-6, 1997
Modane-Avrieux Center
ONERA

DISCLAIMER

Introduction

Large scale structures (LSS) in free-shear mixing layers were first observed by Brown and Roshko (Ref. 1), and by Winant and Browand (Ref. 2). The presence of such large, quasi-periodic structures in mixing layer flows came as a surprise. These early observations were made in very low speed, low Reynolds number flows using planar geometries. Since that time, it has been shown that such large scale structures are intrinsic characteristics of **all** free shear mixing layers, including compressible mixing layers, for any geometry, and at all Reynolds numbers. Further, it is generally accepted (Ref. 3) that these structures dominate the physics of the mixing process, and therefore have enormous cost and performance implications for a wide range of fluid-system technologies. It is noted that essentially all of the fluid systems of significant commercial or military importance operate at high Reynolds numbers, and many, if not most, involve compressible flows. Physically, the large-scale structures are organized, repetitive eddies (vortices) of dimension comparable to the mixing layer thickness.

There currently exists a lack of accurate and robust theoretical models for predicting the formation and character of large scale structures in turbulent free shear layers, even for incompressible flows. This lack severely limits progress in a wide range of important technological areas. As suggested above, the LSS govern the mixing process, with significant implications for fuel efficiency, and gas-phase and particulate pollutant generation in reciprocating, jet turbine, and rocket engines and in stationary combustors. Advanced manufacturing techniques that utilize jet flows, such as thermal spraying, could be improved through a better understanding of turbulent jet mixing. The physical scales and velocities of the LSS determine the frequency and intensity of jet acoustic noise, with significant implications for jet engine marketability. Large-scale turbulent structures play an important role in optical and IR signatures of jet engine exhausts and rocket plumes, of significance in minimizing vulnerability of aircraft or rockets to optical and heat-seeking missiles. Present design methodology uses empirical codes and extensive trial and error, an expensive and inefficient engineering approach. Our goal has been to develop a robust, computationally-efficient predictive model for LSS evolution that is less dependent on empiricism.

This paper is a description of work-in-progress. It describes Sandia's program to study the basic fluid mechanics of large-scale mixing in unbounded, compressible, turbulent flows, specifically, the turbulent mixing of an axisymmetric compressible helium jet in a parallel, coflowing compressible air freestream. Both jet and freestream velocities are variable over a broad range, providing a wide range mixing layer Reynolds number. Although the convective Mach number, M_c, range is currently limited by the present nozzle design to values of 0.6 and below, straightforward nozzle design changes would permit a wide range of convective Mach number, to well in excess of 1.0 The use of helium allows simulation of a hot jet due to the large density difference, and also aids in obtaining optical flow visualization via schlieren due to the large density gradient in the mixing layer. The work comprises a blend of analysis, experiment, and direct numerical simulation (DNS). Here we discuss only the analytical and experimental

efforts to observe and describe the evolution of the large-scale structures. The DNS work, used to compute local two-point velocity correlation data, will be discussed elsewhere (Ref. 4).

Since their discovery, large-scale structures in free shear layers have been studied extensively, both for their intrinsic interest and for the inpact they have on the technologies noted above. Much of the earlier work was directed toward incompressible flows in planar geometries, see for example the review by Ho and Huerre (Ref. 5), and more recently in axisymmetric configurations, by Panchapakesan and Lumley (Ref. 6). Compressible flows in planar 2-D geometries have been investigated by Papamoschou and Roshko (Ref. 7), Arnette, et al, (Ref. 8), Ng, et al (Refs. 9,10), among others. Much of the most recent work has been directed to compressible flows in axisymmetric geometries. Examples are the studies by Pitts (Ref. 11), Clemens and Paul (Ref. 12), and Gutmark and coworkers (Refs. 3, 13-15)

The advantage of a planar geometry is simplicity of flow system design and optical diagnostics. The primary disadvantage of planar 2D geometries is that many practical flow systems are axisymmetric. As a result certain instability modes which are important to the mixing process, the helical modes in particular, are absent. In addition, it is very difficult in general to totally eliminate edge effects, and allegedly planar, 2D flows are in reality always three dimensional to some extent. Flows in axisymmetric geometries are not locally 2D, either. The interaction of axial and helical modes yields strong locally-3D effects. These flows are highly time-dependent in a fixed reference frame. However, the mean (i.e., time-averaged) flows can be, and in fact usually are, axisymmetric 2D.

Gutmark and his coworkers (Refs. 13-15) have studied a compressible, axisymmetric jet of air in coflowing air. This work yielded the first images of large scale structures in supersonic axisymmetric mixing layers. Gutmark, et al., were unable to obtain kinematic data from their experiment, however, and were limited by system design to a small number of freestream and jet Mach numbers. Hence, it would be difficult to generalize their results or to use them for analytical model development. A synopsis of the approach we are taking in the analytical model development is presented in the next section.

Analytical Model Development

The observation that a wide range of shear flows contain quasi-periodic, large-scale structures raises the natural question: can the temporal and spatial evolution of such structures be predicted analytically? Over the last two decades, a small number of engineers and scientists have been working to develop simple, robust, analytical models of the large-scale structures found in the initial mixing region of free-shear flows. The initial mixing region of both shear flows and jets has been the focus of the development of theoretical models because the LSS in the initial mixing region of these flows carry most of the total flow energy and are observed to be approximated by linear models. On the other hand, the LSS found in bounded shear flows and free-shear flows downstream of the initial mixing region have received less attention. This is because these flows tend

to distribute the flow energy across several scales of motion and require nonlinear methods.

The usual goal of a numerical simulation of turbulence is to approximate the mean flow properties, say, pressure and velocity. The mean flow properties are governed by the long-time averaged Navier-Stokes (NS) equations which contain unknowns called the Reynolds stresses. The Reynolds stresses are given by gradients of second order moments of the unsteady flow velocity. Because the Reynolds stress terms are not known *a priori* and are necessary in order to solve the long-time averaged NS equations, these terms must be modeled before the mean properties can be computed.

The traditional approach to solving the mean flow properties is to combine physical scaling ideas with various forms of the equations of motion to generate systems of equations to describe the Reynolds stresses. The combination of scaling and the equations of motion introduces unspecified empirical constants into the expressions used to approximate the Reynolds stresses. The empirical constants are then determined from physical experiments on specific turbulent flows. For those flows, the resulting empirical theory of turbulence can provide very reasonable engineering approximations.

Although the traditional engineering approach is very useful, it has a number of fundamental limitations. This semiempirical theory requires flow-field-specific experimental data. As a result, a turbulence model that works well for one flow may produce highly erroneous results for another. Moreover, different turbulence models can require different physical information. The experimental data needed to approximate the Reynolds stresses can be specific to both the flow and the turbulence model. Probably the largest limitation with the traditional approach is that it does not provide a mathematical prediction; the answer always depends to some degree on experimental observation. Indeed, for many flows the classical semiempirical "theory" reduces to little more than clever statistical curve fits of experimental data.

The fundamental assumption made in the present work is that a deterministic model of the temporal and spatial evolution of the large-scale structures in the coflowing helium/air jet will yield approximations of the Reynolds stress terms, allowing an accurate solution of the long-time averaged Navier-Stokes equations. A model of the Reynolds stresses based on a description of the large-scale motions would yield a semiempirical theory that relies on dimensional analysis and experimental data. However, this approach describes more of the basic physics of turbulence than the traditional engineering method and therefore requires less empiricism. We believe that a successful phenomenological model of the LSS in the coflowing helium/air jet could be extended to predict the evolution of the LSS in jets of arbitrary cross-sectional geometry and for flow conditions outside the range of the experimental parameters used to formulate the model, without resorting to additional experimental input.

In the present research, two analytical approaches are being used to study the LSS in the initial mixing region of the helium/air jet: hydrodynamic stability theory and dynamical systems theory. The basic idea from hydrodynamic stability theory is to describe the unsteady fluctuations associated with the LSS in the jet as a wave in both space and time. To this end, the unsteady pressure and velocity, p' and $\underset{\sim}{u}'$, of the flow are assumed to take the functional form:

$$p'(r,\theta,z,t) \approx A(z)\hat{p}(r,\theta)\exp(i\{\alpha z - \omega t\}) \tag{1}$$

$$\underset{\sim}{u}'(r,\theta,z,t) \approx A(z)\hat{\underset{\sim}{u}}(r,\theta)\exp(i\{\alpha z - \omega t\}) \tag{2}$$

where z is the streamwise direction of the flow and r and θ are the cross-stream directions. In Eqs. (1) and (2), α is a complex number, while ω is a real frequency. Here, A is the amplitude of the fluctuation. The exponential term in Eqs. (1) and (2) models the LSS as a wave in space and time.

The basic idea from dynamical systems theory is to derive a small system of nonlinear ordinary differential equations (ODE's) describing the temporal evolution of the jet which encodes the jet's spatial evolution. The system of ODE's is developed by assuming that the unsteady velocity fluctuations associated with the LSS in the jet may be expressed in the functional form:

$$\underset{\sim}{u}'(r,\theta,z,t) \approx \sum_{k=1}^{N} a_k(t)\underset{\sim}{\phi}^k(r,\theta,z) \tag{3}$$

This decomposition separates the time and space variables in terms of time-dependent amplitudes a_k and spatial eigenfunctions, $\underset{\sim}{\phi}^k$. References 16 and 17 apply the ideas of hydrodynamical stability theory to model large-scale mixing structures in free shear flows, while Ref. 18 describes the ideas of dynamical systems needed to model such fluid motions.

The current research has three near-term analytical modeling goals: 1) apply the two analytical approaches discussed above to compute the evolution of the large-scale motions in the helium/air jet; 2) compare the computational results of the two approaches to assess the differences of the methods; and 3) benchmark the computational results against the experimental observations made here for the helium/air jet. The long-term goal of this effort is two-fold: 1) obtain the theoretical insight into the physics of the LSS needed for the development of robust numerical models; and 2) develop and implement an example of such a model. It is expected that any resulting model of the LSS will be a conceptual extension of the hydrodynamic stability model described by Eqs. (1) and (2).

The experimental work on the coflowing helium/air jet impacts the analytical model development in two fundamental ways. The mean experimental data will be used directly in the development of a model of the LSS, while the time dependent data will be used to validate the model. The unsteady data will also be used to guide and validate direct numerical simulations being applied in the analytical model development. The dynamical systems representation of the large-scale motions given by Eq. (3) requires the computation of the spatial eigenfunctions $\underset{\sim}{\phi}^k$. These functions are determined from two-point velocity correlations measured in the jet on a fine spatial grid. Since a three-dimensional distribution of two-point velocity correlations is very difficult to measure in a compressible, binary gas jet, DNS results from Kennedy (Ref. 19) are being applied to obtain the spatial eigenfunctions needed by Eq. (3). The time dependent experimental data will be used to check the basic characteristics of the time-dependent DNS data used

to generate the spatial eigenfunctions. Figure 1 shows schematically the interaction of the experimental research with the analytical modeling and DNS in the current work.

To date, the hydrodynamic stability and dynamical systems models have been derived for compressible, isothermal, two-dimensional jets; these results are outside the scope of this paper, but will be presented in Ref. 4. A direct numerical simulation has been completed and applied to compute the spatial eigenfunctions ϕ^k for a compressible planar jet. In addition, example hydrodynamic stability computations have been performed to approximate the normalized pressure and velocity fluctuations of the large-scale structures.

Experiment

As indicated above, the purpose of the experimental component of this work is to provide mean and kinematic data in the mixing layer, both to guide development of the analytical model and subsequently to provide data for predictive model validation. A flow system and a variety of diagnostic instrumentation have been developed and demonstrated to assist in that effort. It is stressed, however, that the experimental diagnostics development is not yet complete, and acquisition of sufficient data to meet the analytical modeling needs remains a future goal.

Specific experimental data required for model development are (1) the mean mixing layer profiles for velocity (axial component, at a minimum), temperature, pitot and static pressures, and helium/air molar mixing ratio, and (2) kinematic data consisting of the spatial and temporal frequencies, and axial and radial growth rates of the LSS. (In principle, the local velocity data can also be obtained experimentally; we hope to use Particle Image Velocimetry (PIV) in the next phase of the work. If successful, we can reduce the reliance on results of DNS, which at present can only be computed for low Reynolds number flows (i.e., less than a few thousand), due to computer speed and memory limitations. Briefly, for the mean mixing layer profile data we are using a traversing gas sampling/total temperature probe to determine helium/air mole ratio and temperature, and a pitot probe to determine pitot pressure. In addition, we measure jet exit and free stream static pressures and total temperatures. From these data, the local mean axial velocity, temperature, density, and helium concentration can be determined. The kinematic structure frequency and growth rate data can be obtained from real-time, high-speed movies of the structures.

Facility Design

We are using the Sandia 1-ft x 1-ft (30.5 x 30.5 cm)Trisonic Wind Tunnel (TWT) as a test bed for these experiments. The TWT is nearly ideal for these studies because of its high flow quality, ease of component and optical access, widely variable freestream conditions, and low operational cost. In addition, the jet velocity can be varied over wide ranges, such that both jets and wakes can be generated. This capability allows large-scale-structures to be generated and the structure evolution to be studied over a very wide range in both convective Mach number (to study compressibility effects) and mixing

layer Reynolds number, from zero (no shear velocity) to in excess of 500,000. The latter capability is particularly important, since it allows us to generate low mixing layer Reynolds numbers amenable to DNS calculation for validation of currently available DNS code results.

TWT Control & Data Acquisition

In 1996 we replaced our HP-1000 Data Acquisition & Control System (DACS) with a Pentium PC-based system, and now use LabView™ for all tunnel control and data acquisition functions. In addition, we have replaced the manually-controlled pneumatic actuator for the pressure regulating valve (PRV) used for stagnation pressure (P_o) control by a software-controlled hydraulic system. This change has increased PRV frequency response by a factor of about 20, and allows P_o to be maintained constant over a run to within a few tenths of a percent compared to about 1% as previously obtained by a skilled operator using the manually-controlled, pneumatically-actuated PRV.

The fully operational Mach number and stagnation pressure range is achievable with the pipe installed, except there is a slight increase [O(1%)] in test section freestream Mach number at supersonic conditions due to the reduction in effective throat area.

Helium Flow Pipe & Gas System

The pipe OD at the nozzle exit is 31.75 mm and the lip thickness is 0.254 mm. The inner contour is comprised of a hyperbolic tangent profile matched at the nozzle mid-point. Honeycomb (1.6 mm cell, 1.0 cm long) placed upstream of the nozzle throat is used to straighten the flow and to damp large-scale turbulence. The design also allows for installation of screens downstream of the honeycomb, if desired, but screens are not normally used. A flow spreader, of 15% or 30% porosity, is located 1.7 cm forward of the honeycomb.

The flow pipe is 2.16 m long and extends from the TWT test section upstream through the tunnel throat and into the settling chamber, where it is supported by four tensioned rods located just downstream of the turbulence screens. It is supported at the downstream end at a location 31.9 cm upstream of the nozzle exit by four 1.6 mm diam. aircraft control cables arranged in a flattened-X configuration (+/- 37 deg from horizontal). The cables are attached to the test section side walls by threaded fittings which allow pipe alignment in the test section and cable tension control. This design was chosen over a shorter, strut-supported pipe because of the potential effect of the strut on the mixing-layer flow, and the presence of strong shock waves on the forebody at supersonic freestream Mach numbers. The use of a longer pipe with cable supports introduces other concerns, however. These are the effects of the cable wakes (presumed to be oscillatory) on the mixing, and the presence of a thicker boundary layer (estimated to range from 0.25 cm to 1 cm thickness, depending on flow conditions) on the pipe exterior surface as a result of the longer pipe length.

Prior to final machining of the pipe nozzle section a pipe dynamics study using two-axis accelerometers at the pipe midpoint and at the nozzle end was conducted. This study demonstrated that there were no adverse pipe motions for any desired test section

freestream condition. Figure 2 shows a schematic of the TWT with the helium flow pipe installed. Figure 3 is a photo of the TWT with the flow pipe installed and one plenum sidewall removed.

The pipe nozzle is provided with a thermocouple and pressure tap upstream of the honeycomb for jet total temperature and pressure measurement, and a 0.51 mm ID static pressure port 6.35 cm upstream of the nozzle exit.

Standard-purity (99.99%) helium is delivered to the flow pipe from a bottle farm through a high-flow manifold. A high-flow dome-loaded regulator is used to control helium pressure. Except as noted below, all flow lines are 3/4-in (1.9 cm) OD SS tubing to minimize viscous pressure loss. Helium volume flow rate is measured with a 1-in. (2.54 cm) diameter turbine meter with upstream flow straighteners. Pressure and temperature are measured immediately upstream and downstream of the turbine meter; these data are used to convert volume flow rate to mass flow rate of helium. A computer-controlled 1-in. proportioning valve is used to control flow rate, based on a calibration of the flow rate as a function of helium regulator pressure, temperature, and proportioning valve setting. Actuation of the proportioning valve is too slow to vary flow rate during a run so is used in a pre-set mode only. SS tubing (3/4 in.) penetrates the tunnel pressure shell; this line connects to flexible 3/8-in high-pressure line in the settling chamber for connection to the upstream end of the flow pipe. Typical helium mass flow rates vary from 5 to 50 gm/sec and are highly stable. At very high flow rates (100 gm/sec and above), the helium flow becomes unstable, and the flow rate and helium line pressure oscillate severely, a condition which must be avoided. (We are not certain as to the source of the instability. It is probably related either to alternating transition between laminar and turbulent flow in the piping, or to a varying choke point location, or both.) The flow system is shown schematically in Fig. 4.

Flow Visualization

High-speed schlieren. High-speed schlieren is used to image the LSS in real time. These records yield the spatial and temporal frequencies, growth rates, and air/helium interface velocity of the LSS. Schlieren takes advantage of the high density gradient between the air and helium, and yields excellent optical contrast. As discussed further below, these images do not yield kinematic information internal to the mixing layer.

High speed cameras synchronized with a repetitively-pulsed laser light source or a xenon flash lamp are use for schlieren imaging. We use either of two cameras, a Kodak 4540 Ektapro digital camera or a NAC-1000 Super-VHS camera. The Kodak is used to record images at frame rates sufficient to track individual structures, and is required to extract kinematic data. Sufficient memory is available, 320 Mbytes, to store up to 5120 full frame 256 x 256 pixel images. Maximum optical speed is equivalent to ISO 3000 film. A range of fixed frame rates is available from 30 frames per second (fps) up to 40,500 fps. At frame rates over 4500 fps, the images are reduced in size but maintain constant areal pixel density, i.e., constant image plane resolution. Image format varies with frame rate. The images can be post-processed using image motion analysis software. The NAC camera provides schlieren video at up to 1000 fps using a synchronized xenon flash lamp of approximately 3 microsecond pulse duration as a light

source. Image resolution is several times higher than for the Kodak at the same magnification. However, at 1000 fps, individual structures cannot be followed in sequential images, i.e., images are uncorrelated in time. We can also acquire standard 30 fps S-VHS video synchronized with the xenon flash lamp.

An Oxford Lasers Cu-10A 10-watt, variable-pulse-rate copper vapor laser is used to provide the short (10-20 nanosecond) light pulses required to minimize motion blur. (For structure velocities of up 300 m/sec, motion blur is less than 100 microns, which is significantly less than the object plane image resolution.) Laser pulse rate is continuously variable from about 4000 to 23000 pps as presently configured, although output power cannot be maintained constant over extended periods at pulse rates below 5500 pps. (Pulse rates up to 32000 pps can be obtained with modifications to the laser power supply.) Laser output power is a function of pulse rate. Output power peaks at 10 watts at 10KHz, and decreases monotonically at higher and lower pulse rates. At 6 and 18KHz, output power is reduced by about 40%.

A 1-mm fiber optic cable is used to transport the laser output to the schlieren system. Typically, laser pulse rates of 4500, 9000, and 18,000 pps are used to match available recording speeds of the Ektapro camera. Of these, the 18,000 fps is the most useful since the camera image shape, a rectangle of aspect ratio four, best matches the proportions of the jet flow and also provides the finest temporal resolution. For the lower LSS velocities, we are able to track individual structures in sequential images at the 4,500 frame rate. At the highest velocities, the 18,000 fps rate is required. Synchronization between the laser and either camera is achieved by triggering the laser with a camera output pulse.

In general, the laser power available, even after delivery by the fiber optic, is far greater than needed for schlieren. We attenuate the laser by a factor of 100 using a remotely-controllable mechanical attenuator, then further attenuate the light by another factor of ten using neutral density filters. The schlieren system is shown schematically in Fig. 5. A typical example of Kodak (laser light source) or an NAC (xenon light source) image is shown in Fig. 6, for a Mach 0.1 He jet in a Mach 1.2 air freestream.

Laser Light Sheet/Flow Seeding. As indicated above, schlieren is excellent for general imaging of the structures. However, it is known that the flow within the mixing layer is three-dimensional due to the interaction of axial and helical instability modes. Schlieren, being a two-dimensional imaging technique, integrates along a line of sight through the jet. To observe the character of the flow inside the mixing layer, another technique is required. We have considered two alternate approaches: focusing schlieren (Ref. 20) and use of a laser light sheet with seeding (Ref. 21). We have opted to pursue the laser light sheet with seeding since that approach also supports PIV measurements (Ref. 21).

A laser light sheet optical system was designed and constructed using a 1 mm optical fiber to deliver the light to the tunnel test section, and a 6 mm focal length cylindrical lens to spread the beam. The system is shown schematically in Fig. 7 in relation to the tunnel. The lens is flat on one side, with the flat side flush with the tunnel floor. On the flat surface is a 0.5 mm wide slit, to confine the light to a relatively narrow sheet. The light sheet has a thickness of 3-4 mm at a height 15 cm from the lens, and spreads in a fan of approximately 45 degrees full angle, yielding an illuminated region

along the jet axis approximately 12 cm in length. The lens holder penetrates and is mounted to the tunnel floor, and can be rotated to change the orientation of the sheet with respect to the flow: parallel to, normal to, or at 45 degrees to the jet. The lens holder can also be moved to different axial stations in the tunnel test section to image different portions of the jet.

Since laser power density in the sheet is far too low to allow the Rayleigh scattering by the helium or air molecules to be imaged, the laser light sheet approach requires that either the jet or the air freestream be seeded with light scattering particles. At the suggestion of researchers at NASA Langley (Ref. 22), we have been attempting to use polyethylene glycol (PEG)/water mixtures as the seeding agent. PEG has a very low vapor pressure, dissolves completely in water at any concentration, is available in a range of molecular weights, viscosities, and dew points, is non-hazardous in the low quantities required, and residue can be wiped clean using water. Therefore, this material combination is very attractive in principle for seeding flows of the type studied here. (The option of using fluorescent compounds as a particulate or gaseous seed is not easily available to us; nearly all such compounds are toxic, creating an environmental and health hazard, and also typically require a UV excitation source, a safety concern.)

To date we have been unable to obtain usable images. There appear to be several reasons for this. First, light sheet intensity is now a dominant factor. The 1 mm fiber is able to deliver only 0.5 watt into the sheet due to the focusing limits imposed by the large fiber diameter combined with other geometric constraints. We are pursuing the use of a 0.3 mm diameter fiber and a modification to the sheet-forming lens system to improve the ability to focus in an attempt to alleviate this limitation. With these changes, we hope to increase the power into the sheet by a factor of up to 5.

The other limiting factor is the seed diameter and particle density. For visualizing the overall structure characteristics internal to the jet, we desire a dense fog of very small light-scattering particles. A fundamental problem with seeding high speed flows is that the high fluid velocity spreads the particles out, reducing the instantaneous scattered light per unit area. In addition, if attempting to track (larger) individual particles in the flow, such as for PIV applications, particle velocity lag must be considered. Clearly, for a given total seeding rate, there is a trade-off between particle size and number density. For visualizing the structures, a fog of smaller droplets is preferred; for PIV, a smaller number of larger particles is required.

The seeding system is shown schematically in Fig. 8 and in the photograph of Fig. 9. PEG/water droplets are formed by a 0.06 mm diameter simplex spray nozzle via direct injection into the helium flow at high pressure, 200-900 psig (1.4-6.2 MPa). The water evaporates in the dry helium, creating a spherical PEG particle of reduced size. The final diameter, d_f, compared to the original droplet diameter, d_i, is a function of the initial concentration, C, i.e., $d_f/d_i=C^{1/3}$. For our application, the droplets must be created outside the tunnel, then carried with the helium through the pipe, a distance of more than three meters. For this to be successful, very small droplets that can follow the flow so as to avoid contact with the pipe wall, honeycomb, etc., are required. Calculations based on particle size correlations in Ref. 23 indicate that for injection pressures of several hundred psi, droplets in the 1-10 micron range should be produced by our system. For a typical concentration of 15% PEG by volume in water the final droplet diameter is expected to

be approximately 0.5-5 microns. The smaller of these were expected to follow the flow and to be produced in sufficient numbers to be seen as a fog. Indeed, we observe what appears to the eye to be a nearly uniform fog at the nozzle exit. Further, we note that with the plane of the light sheet oriented perpendicular to the flow, intensity is sufficient to make the flow visible in the CCD camera images. Since the total intensity at a point in the camera image increases by a factor of about six for this sheet orientation relative to that with the sheet parallel to the flow, we are hoping that the change in fiber optic system alone will be sufficient to yield usable images. At the same time, we are continuing to try to improve the seeding system efficiency.

Aspirating Gas Sampling Probe

An aspirating gas sampling probe is used to measure the helium concentration. The design is based on the aspirating probe developed by Ng, et al., (Refs. 9 & 10) for supersonic flow. It is also applicable to subsonic flow, although the spatial resolution decreases since the probe will sample a larger effective volume around the tip. The probe is depicted schematically in Fig. 10. Figure 11 is a photograph of the completed probe shown in the wind tunnel. Fluid from the mixing layer is drawn into the probe through the tip, and exits the probe through a downstream choked orifice of larger diameter connected to vacuum. If the flow into the probe is supersonic, the sharp, conical tip "swallows" the stream-tube, and the flow undergoes a Prandtl-Meyer expansion to still higher Mach number inside the cone. A strong normal shock forms at some point upstream of the hot film, with the shock location depending on the pressure in the probe relative to the mixing layer, and the Mach number inside the probe tip. The flow continues to decelerate to nearly zero Mach number in the subsonic diffuser downstream of the shock. It then passes over a 0.002-in. (.050 mm) diam x 0.040-in. (1.0 mm) long hot film element (TSI Model 10121-20), and through the downstream choked orifice. The choked orifice dictates the mass flow for given mixing layer and probe pressures, and it is essential that sufficient vacuum be applied to ensure that the choke point is at the downstream orifice.

The design concept of the probe is that the heat transfer from the hot film is a function of the velocity, density, and composition of the flow across it. For given velocity and density, helium has a larger effect than does air; hence, probe output increases with increasing helium concentration. For nearly stagnant flow in the vicinity of the hot film, the contribution due to velocity is negligible.

The hot film is operated in the constant-temperature mode at an overheat ratio of 0.6. The (total) pressure and temperature adjacent to the hot film are measured. Hence, the hot film voltage is a function of pressure, temperature, and helium concentration. A Dantec Model 90N10 digital hot wire anemometer system is used to acquire and analyze the hot film signals. Digital integration over several LSS cycles is required to obtain stable data. Calibration of the probe output is achieved by operating the probe in a static tank containing helium-air mixtures of known, and variable, helium concentration, pressure, and temperature. The calibration procedure is computer-controlled, so as to permit a series of calibrations to be automatically acquired over a range of helium concentration, and tank pressure and temperature. A typical probe calibration as a

function of probe pressure P_1 and helium concentration X_{He} at a tank temperature of 300K is shown in Fig. 12. It is noted that significant care is required in the probe mechanical design, especially the tip/hot film region, to ensure the probe operates as intended. If the shock wave in the tip stands too downstream, then there will be a significant contribution of velocity to probe output. Since the location of the shock is not fixed, the actual velocity at the hot film will vary widely, and the probe cannot be accurately calibrated.

For our initial concentration measurements in the jet mixing layer, the probe was mounted on the TWT pitching strut and pitched through a range of angle of attack from 0 up to 14 deg at an axial location 64.3 mm from the nozzle exit. Profiles of helium concentration in the mixing layer, obtained as a function of jet radius using the pitched probe, are shown in Fig. 13 for freestream Mach numbers of 0.5, 0.9, and 1.3.

The probe concentration measurement accuracy is reduced slightly if the probe is at an angle of attack in supersonic flow (Ref. 9). Both to avoid this error and to allow us to sample the entire jet volume, we have designed and are now attempting to implement a software-driven probe traversing mechanism that will translate the probe across the jet while maintaining the probe axis parallel to the flow. Translational speed is 2 cm/sec and the mechanism can be rotated through 360 deg at fine azimuthal increments to permit any part of the jet (for example, the wakes of the pipe support cables) to be studied in detail. A photo of the individual components of this mechanism is shown in Fig. 14.

As noted above, a complete description of the flow requires that the pitot pressure, static pressure, and stagnation temperature also be known as a function of position in the mixing layer. For subsonic freestream Mach numbers, the jet exit static pressure is very nearly equal to the tunnel freestream pressure, which is presently measured separately at a location on the test section wall. (This approximation worsens at supersonic freestream Mach numbers; for these conditions, we will measure the static pressure in a separate run using a 5-hole probe.) Stagnation temperature is determined from the gas sampling probe thermocouple. The stagnation temperature varies with radial position in the jet, since the jet and freestream stagnation temperatures are different, $\approx$295K and $\approx$340K, respectively. In addition the apparent stagnation temperature, as measured by the probe, is slightly elevated (3-6K) relative to the true gas stagnation temperature due to the heat input from the hot film; however, this error cancels out in the calibration process. The probe pressure P_1 is <u>not</u> the pitot pressure, since the flow has been processed by a strong shock inside the probe. Therefore, pitot pressure must also be measured independently. In future work we plan to obtain pitot pressure using one or more pitot probes attached to the forecone of the mass sampling probe, with the pitot probe tip(s) located as close as practical to the gas sampling probe tip orifice. By this means we hope to avoid the need to measure pitot pressure in a separate tunnel run.

Results and Conclusions

We have successfully demonstrated reliable, stable operation of the helium jet in a coflowing air freestream over a wide range of jet and freestream conditions. There are no adverse flow pipe dynamics at any operating condition. Excellent schlieren movies of the

mixing layer have been obtained in real time at up to 18,000 frames per second using a repetitively-pulsed laser in synchronization with a high speed digital CCD camera. From these images, the velocity, spatial and temporal frequencies, and growth rates can be extracted. The ability to measure mean helium molar concentration as a function of radial position in the mixing layer has been demonstrated over a range of freestream Mach numbers using an aspirating gas sampling probe.

The evolution of the large scale structures observed here is qualitatively in agreement with recent results for similar shear velocities between a circular air jet and coflowing air freestream (Refs. 13-15). At the lower shear velocities seen in our experiments, the structures are larger, more well defined, and highly periodic. As shear velocity increases, the structures decrease in size, increase in spatial frequency, and become less regular. The mean helium mole fraction profiles shown in Fig. 12 suggest that the mixing improves with increasing shear velocity as evidenced by the broadening of the profile and the more rapid encroachment of the profile median point into the jet core. This is in qualitative agreement with the observed increase in *planar* mixing layer growth rate with shearing velocity as discussed by Messersmith, et al., (Ref. 24). We have not yet acquired the data required to assess the role of compressibility in our axisymmetric shear layer; the work by others for plane shear layers suggests the effect of compressibility may be similar to that of shear velocity, i.e., increasing convective Mach number tends to reduce radial growth rates and decreases the regularity of the structures. As discussed by Clemens and Paul (Ref. 12), however, the role of compressibility in LSS evolution in axisymmetric free shear layers is not yet clear.

Large-scale structure velocities have been determined in a few cases from the video images. These results are heavily biased toward the coflowing freestream velocity, however, due to the character of the schlieren technique, that is, only the edge of the shear layer can be unambiguously identified. At all other locations, one is viewing a two-dimensional projection along a line of sight through the jet. In general, the measured LSS edge velocities are very close to the calculated freestream velocity for the particular flow condition. As discussed above, velocity data internal to the jet must be obtained from the seeded laser light sheet images, which are not yet available.

Future Work

This work continues. During the summer of 1997 we hope to improve the laser light sheet/seeding system so as to obtain images of the large scale structures interior to the jet. In conjunction with that effort, we may have an opportunity to use PIV to determine the two-component velocities within the LSS, and if successful, to use these data in the analytical model development work. We also hope to demonstrate the traversing mechanism/gas sampling probe system, and to use the data to assess the effects of the support cables. Whether the work will continue beyond FY97 depends on upcoming funding allocation decisions.

Acknowledgements

The authors gratefully acknowledge the assistance of the following Sandia National Laboratories personnel: J. F. Henfling for software development and wind tunnel operation, C.B. Lafferty for facility support,of the, D.L. Preston for the flow pipe design, and M.W. Pilcher for the design of the probe and probe traversing mechanism.

This work was supported by the US Department of Energy and Lockheed Martin Corporation under contract DE-AC04-94AL85000.

References

1. G.L. Brown and A. Roshko, "On Density Effects and Large Structures in Turbulent Mixing Layers", *J. Fluid Mechanics*, 64, pp. 775-816, 1974.

2. C.D. Winant and F.K. Browand, "Vortex Pairing: The Mechanisms of Turbulent Mixing Layer Growth at Moderate Reynolds Numbers", *J. Fluid Mechanics*, 63, pp. 237-255, 1974.

3. E. Gutmark, T.P. Parr, D.M. Hanson-Parr, and K.C. Schadow, "Coherent and Random Structure in Reacting Jets", *Experiments in Fluids*, 10, pp. 147-156, 1990.

4. D.P. Aeschliman, R.S. Baty, and C.A. Kennedy, "Large-Scale Structures in Turbulent Free-Shear-Layer Mixing", Sandia National Laboratories Report, in preparation.

5. C.-M. Ho and P. Huerre, "Perturbed Free Shear Layers", *Ann. Rev. Fluid Mechanics*, 16, pp. 365-424, 1984.

6. N.R. Panchapakesan and J.L. Lumley, "Turbulence Measurements in Axisymmetric Jets of Air and Helium', *J. Fluid Mechanics*, 246, pp. 225-247, 1993.

7. D. Papamoschou and A. Roshko, "The Compressible Turbulent Shear Layer: An Experimental Study", *J. Fluid Mechanics*, 197, pp. 453-477, 1988.

8. S.A. Arnette, M. Samimy, and G.S. Elliott, "The Effect of Expansion on the Large-Scale Structures of a Compressible Turbulent Boundary Layer", AIAA Paper 93-2991, 24th Fluid Dynamics Conf., July 1993.

9. T.A. Ninnemann and W.-F. Ng, "A Concentration Probe for the Study of Mixing in Supersonic Shear Flows", *Experiments in Fluids*, 13, pp. 98-104, 1992.

10. W.-F. Ng and A.H. Epstein, "High-Frequency Temperature and Pressure Probe for Unsteady Compressible Flows", Rev. Sci. Instruments, 54, pp.1678-1683, 1983.

11. W.M. Pitts, "Effects of Global Density Ratio on the Centerline Mixing Behavior of Axisymmetric Turbulent Jets", *Experiments in Fluids*, 11, pp. 125-134, 1991.

12. N.T. Clemens and P.H. Paul, "Scalar Measurements in Compressible Axisymmetric Mixing Layers", AIAA Paper 93-0220, 31st Aerospace Sciences Mtg, 1993.

13. K.H. Yu, E. Gutmark, R.A. Smith, and K.C. Schadow, "Coherent Vortex Formation in Compressible Shear Layers of Supersonic Coaxial Jets", 9th Symposium on Turbulent Shear Flows, Kyoto, Japan, Aug. 1993.

14. E.Gutmark, K.C. Schadow, and K.H. Yu, "Mixing Enhancement in Supersonic Shear Flows", *Ann. Rev. Fluid Mechanics*, 27, pp. 375-417, 1995.

15. K.C. Schadow, E. Gutmark, and K.J. Wilson, "Compressible Spreading Rates of Supersonic Coaxial Jets", *Experiments in Fluids*, 10, pp. 161-167, 1990.

16. C.K.W. Tam and P.J. Morris, "The Radiation of Sound by the Instability Waves of a Compressible Plane Turbulent Shear Layer", J. Fluid Mechanics, 98, 1980.

17. P.J. Morris, M.G. Giridharan, and G.M. Lilley, "On the Turbulent Mixing of Compressible Free Shear Layers", *Proc. Royal Society, A*, 431, 1991.

18. P. Holmes, J.L. Lumley, and G. Berkooz, *Turbulence, Coherent Structures, Dynamical Systems, and Symmetry*, Cambridge University Press, 1996.

19. C.A. Kennedy, Private Communication, 1996.

20. L.M. Weinstein, "An Improved Large-Field Focusing Schlieren System", AIAA Paper 91-0567, 29th Aerospace Sciences Mtg, Jan. 1991.

21. W.D. Urban and M.G. Mungal, "Planar Velocity Measurements in Compressible Mixing Layers", AIAA Paper 97-0757, 35th Aerospace Science Mtg, Jan. 1997.

22. J.L. Herrin, Private Communication, 1995.

23. A.H. Lefebvre, *Atomization and Sprays,* Hemisphere, 1989.

24. N.L. Messersmith, J.C. Dutton, and H. Krier, "Experimental Investigation of Large -Scale Structures in Compressible Mixing Layers", AIAA Paper 91-0244, 29th Aerospace Sciences Mtg, Jan. 1991.

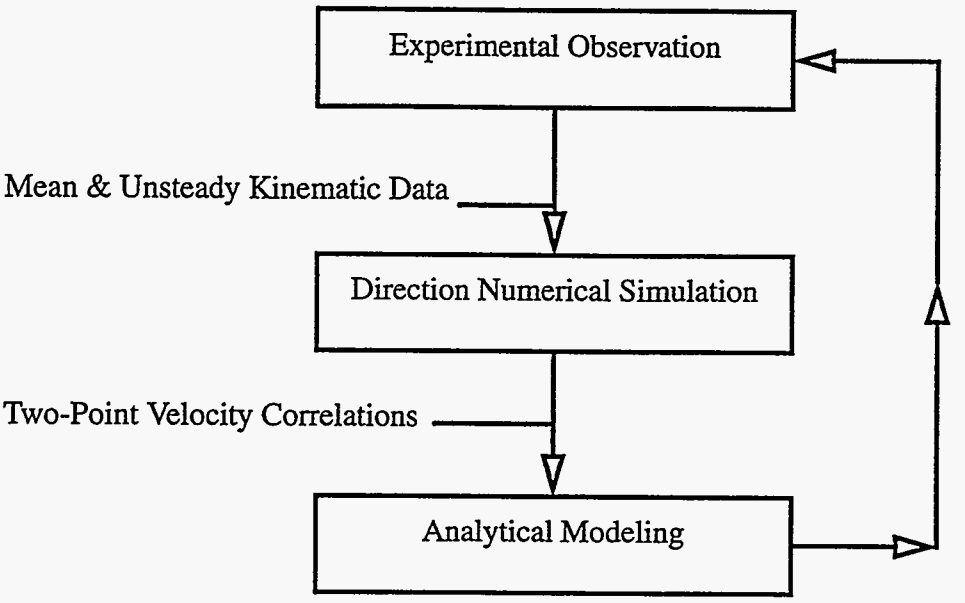

Figure 1. Interaction between analytical modeling, direct numerical simulation, and experiment in the study of large-scale coherent evolution in compressible, axisymmetric free-shear layers.

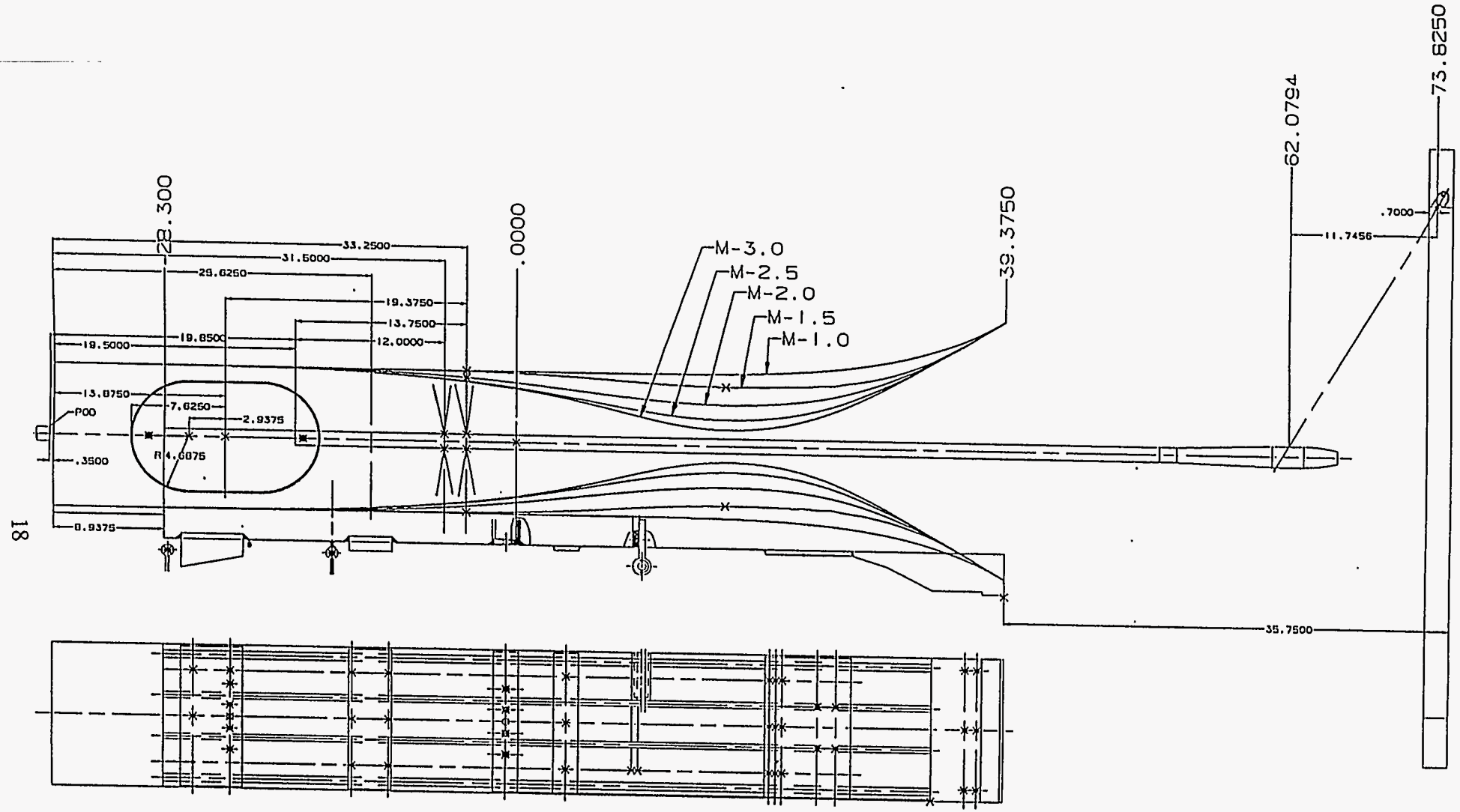

Figure 2. Schematic of Trisonic Wind Tunnel with helium flow pipe installed. Varying wind tunnel nozzle contours are for transonic and supersonic freestream Mach numbers.

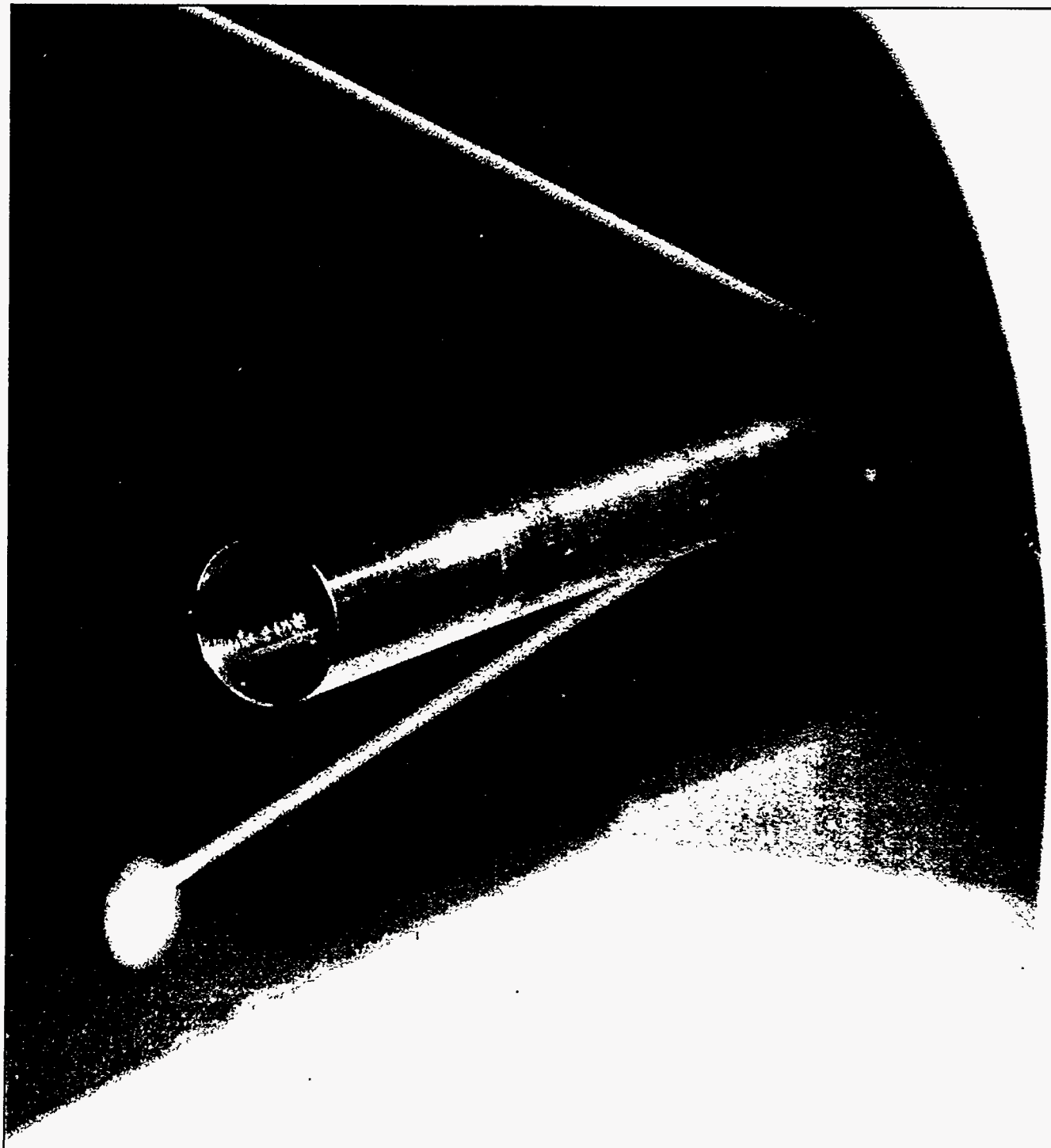

AESCHLIMAN/04-09-97:15

Figure 3. Photograph of the Trisonic Wind Tunnel with helium flow pipe installed and one plenum side wall removed.

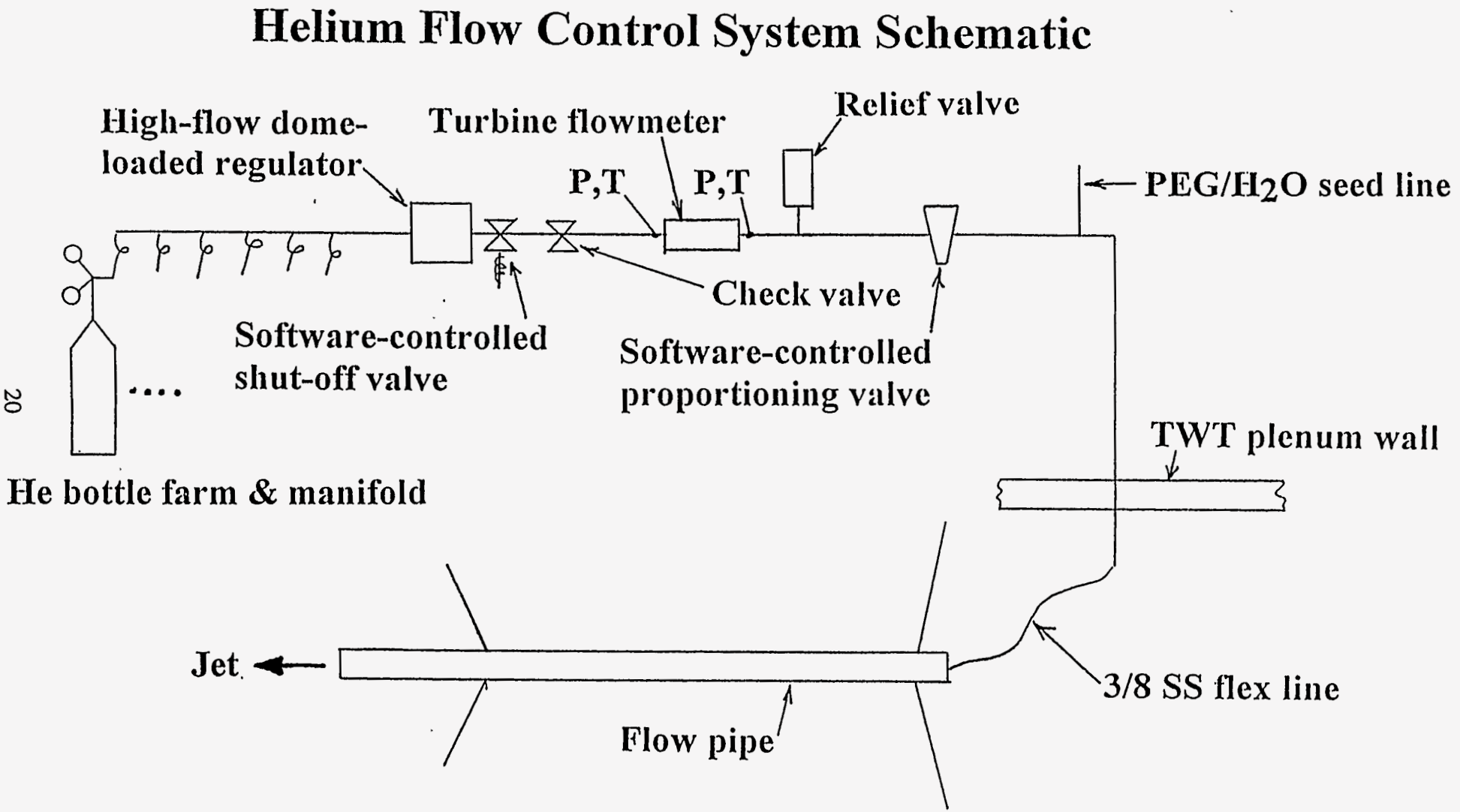

Figure 4. Schematic drawing of the helium flow control system.

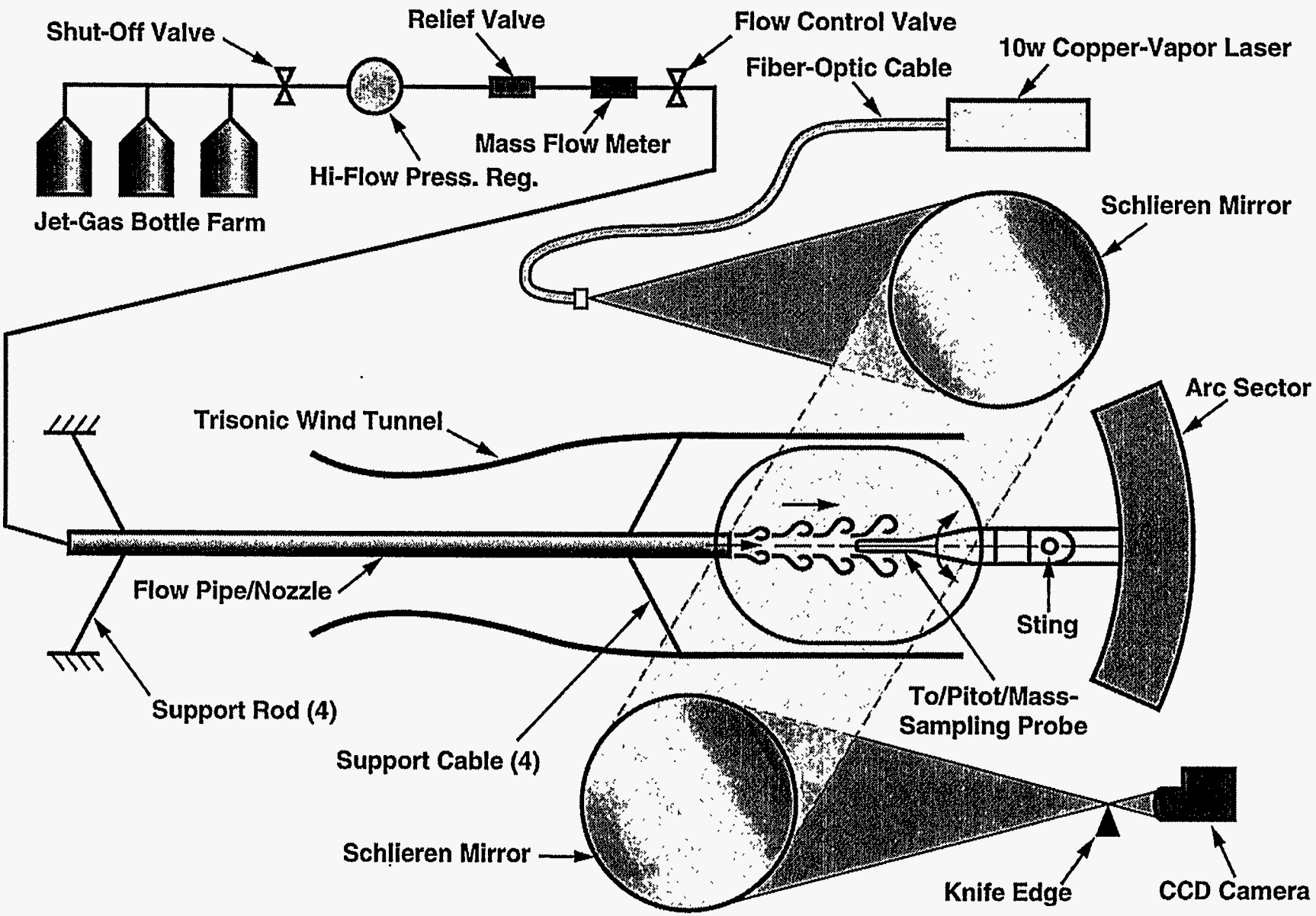

Figure 5. Schematic representation of TWT schlieren system with pulsed laser light source.

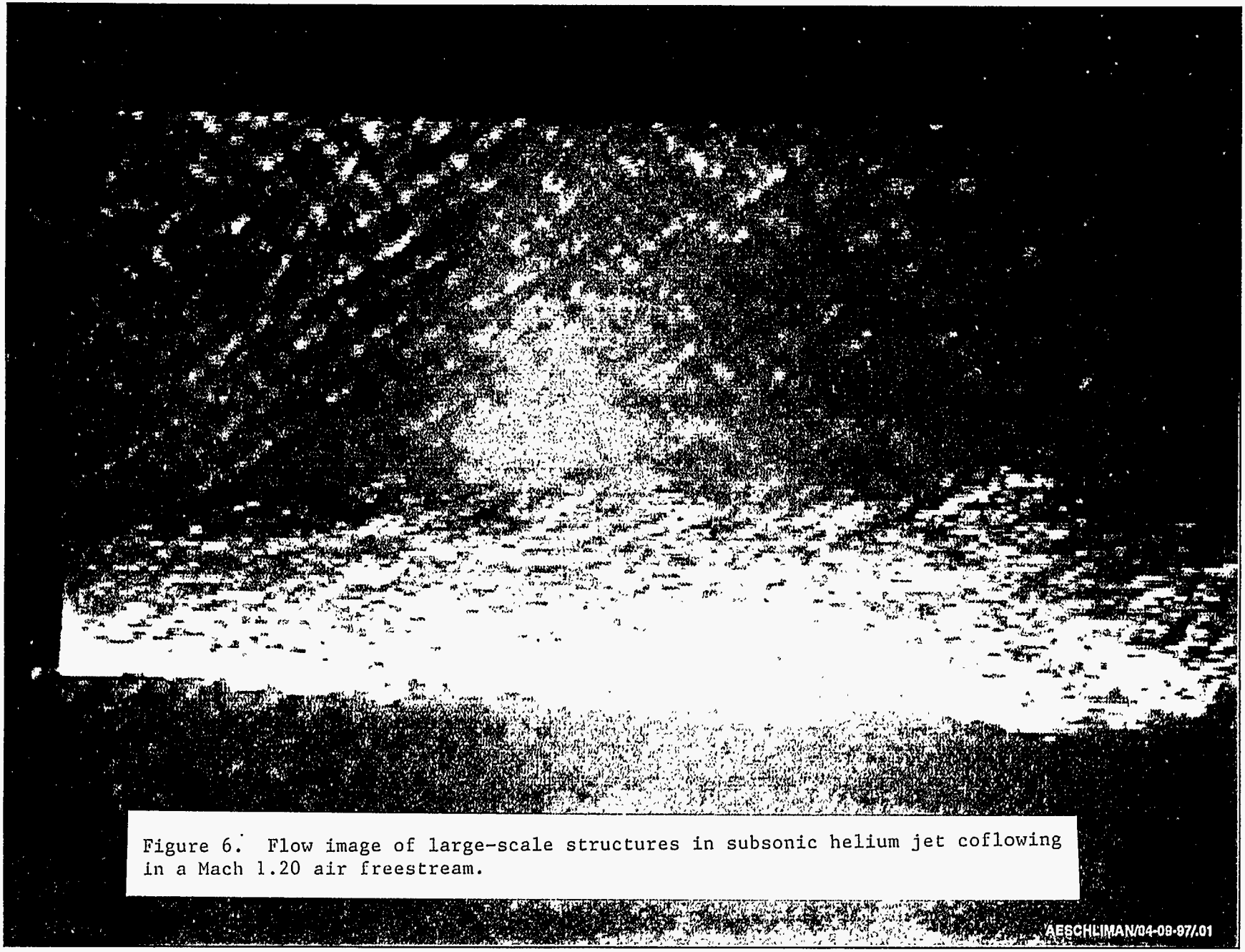

Figure 6. Flow image of large-scale structures in subsonic helium jet coflowing in a Mach 1.20 air freestream.

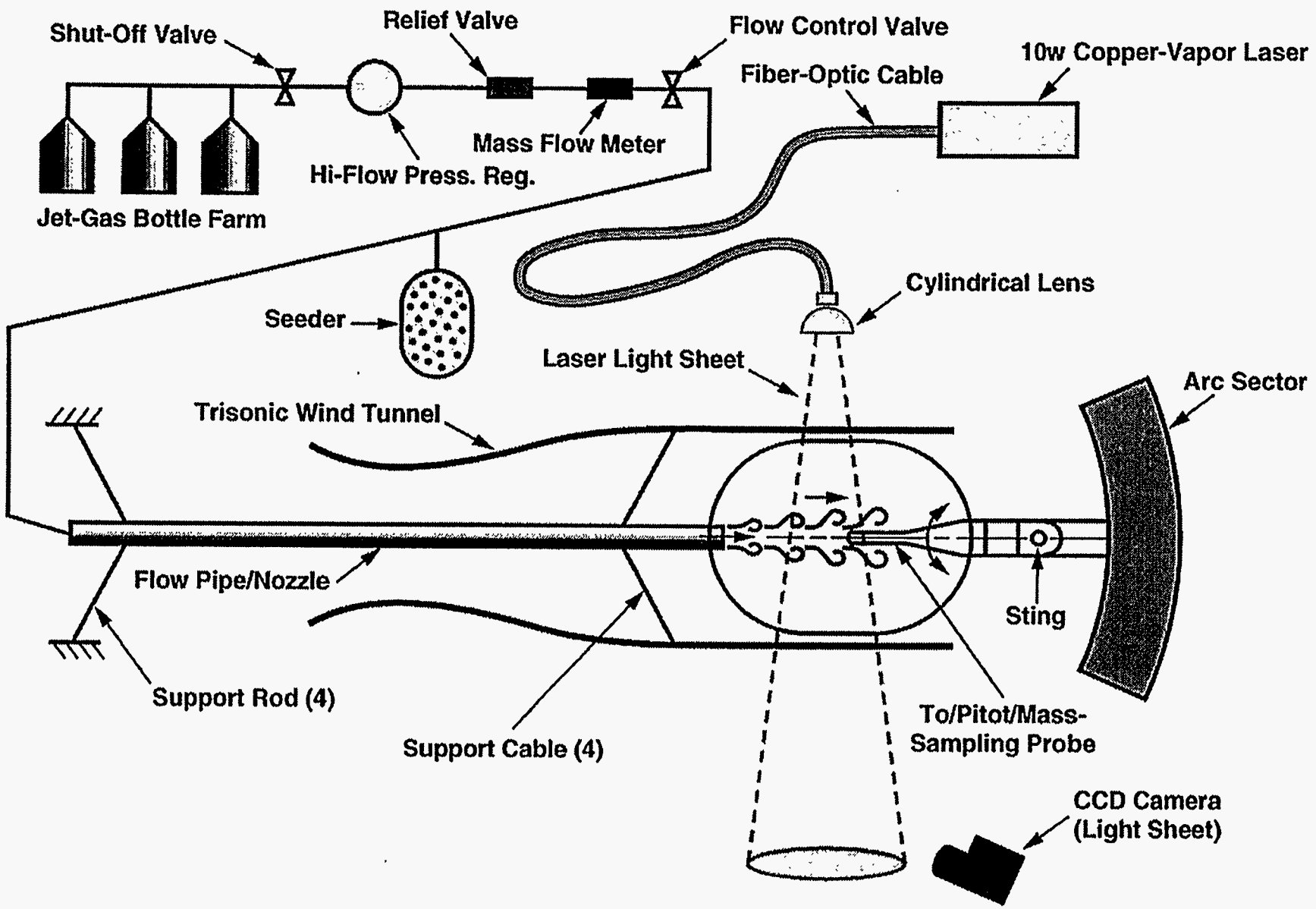

Figure 7. Schematic of laser light sheet/seeding system in relation to tunnel.

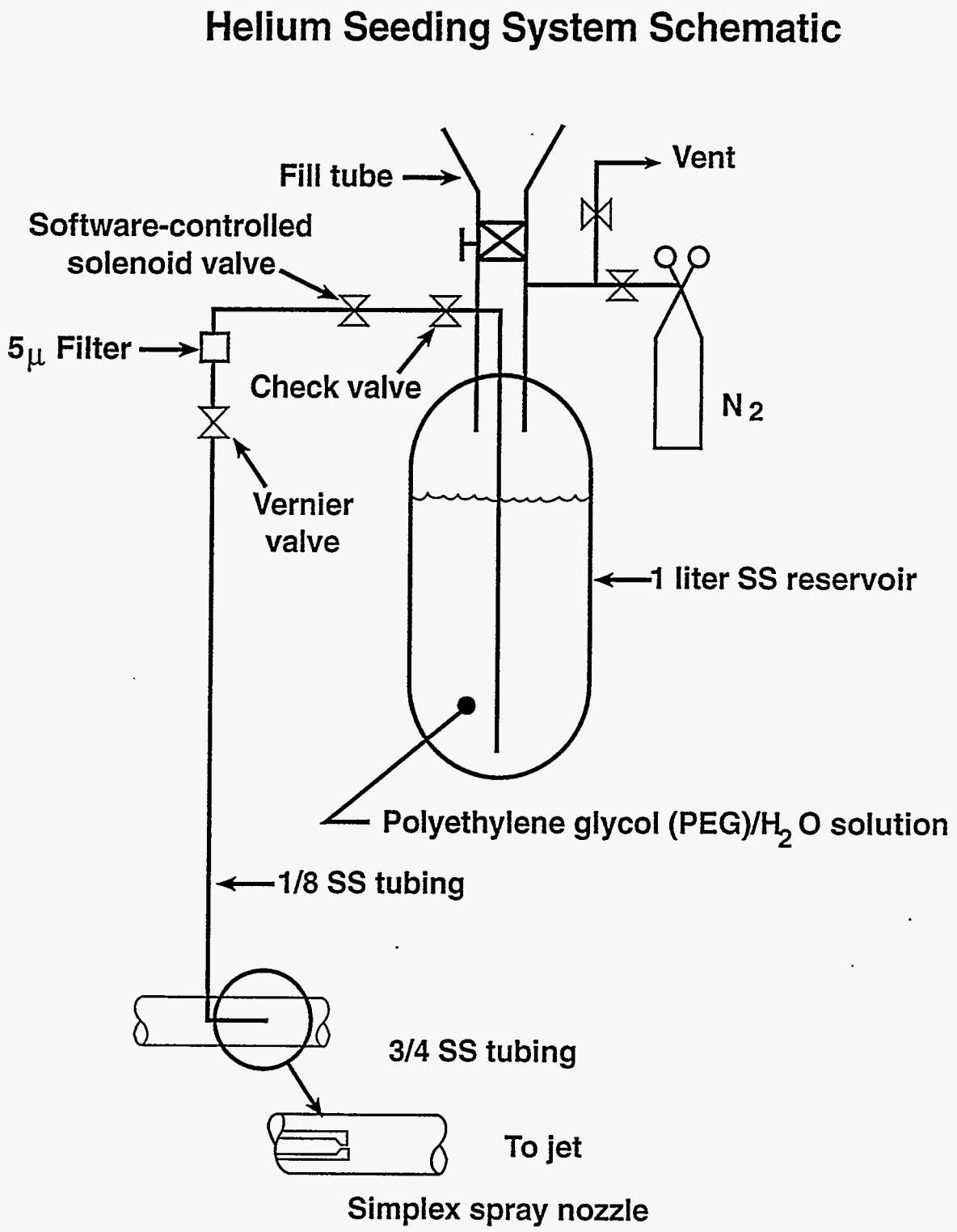

Figure 8. Schematic of helium flow seeding system.

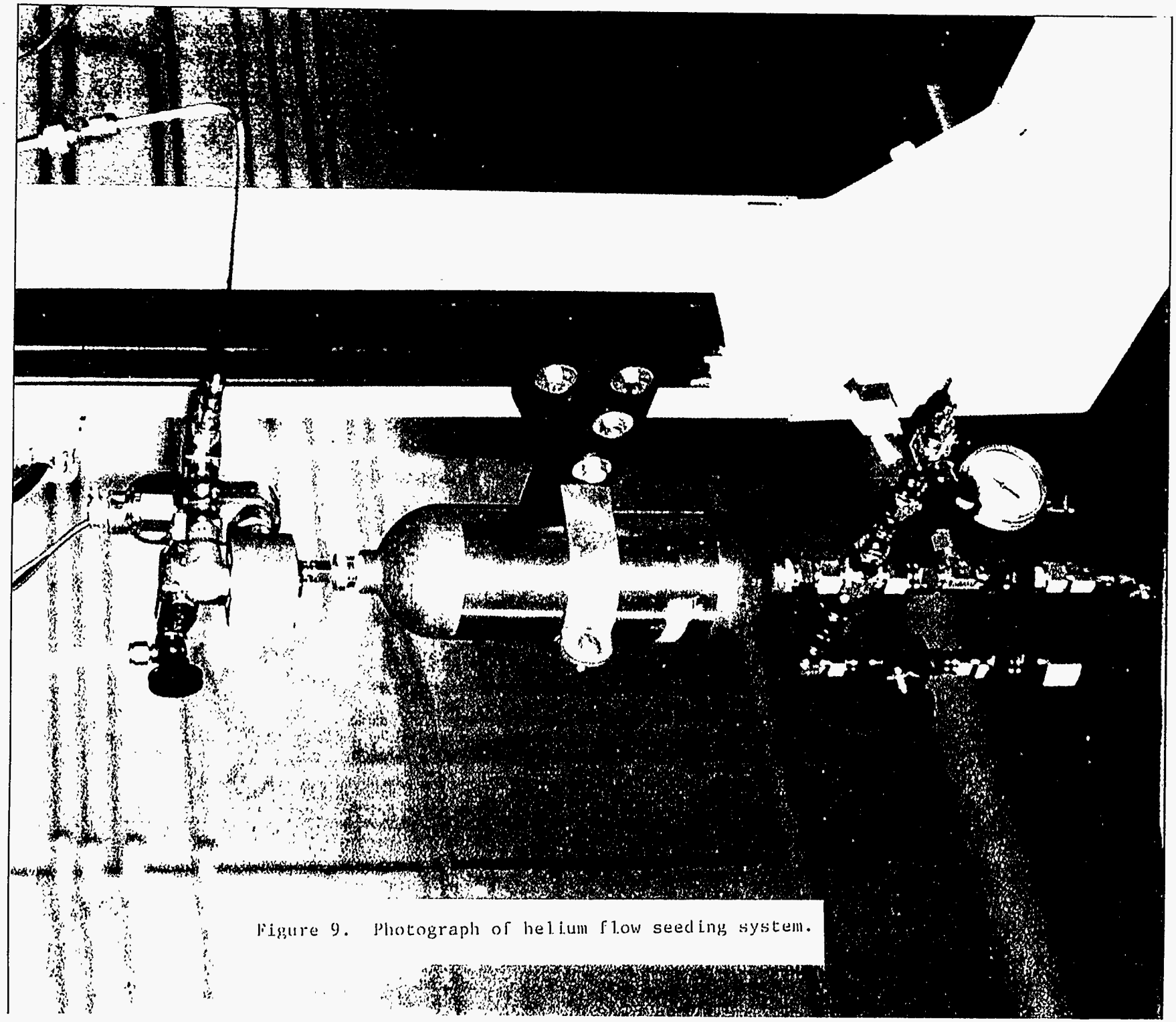

Figure 9. Photograph of helium flow seeding system.

Aspirating Gas-Sampling Probe

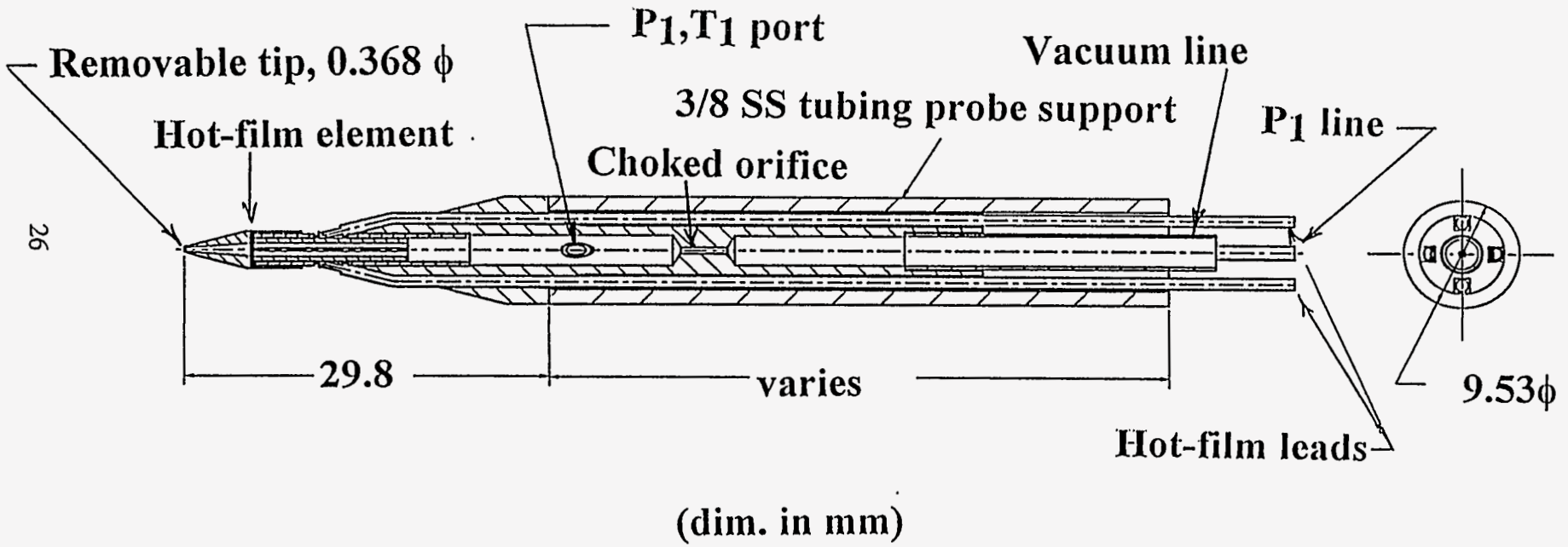

Figure 10. Schematic of aspirating gas sampling probe.

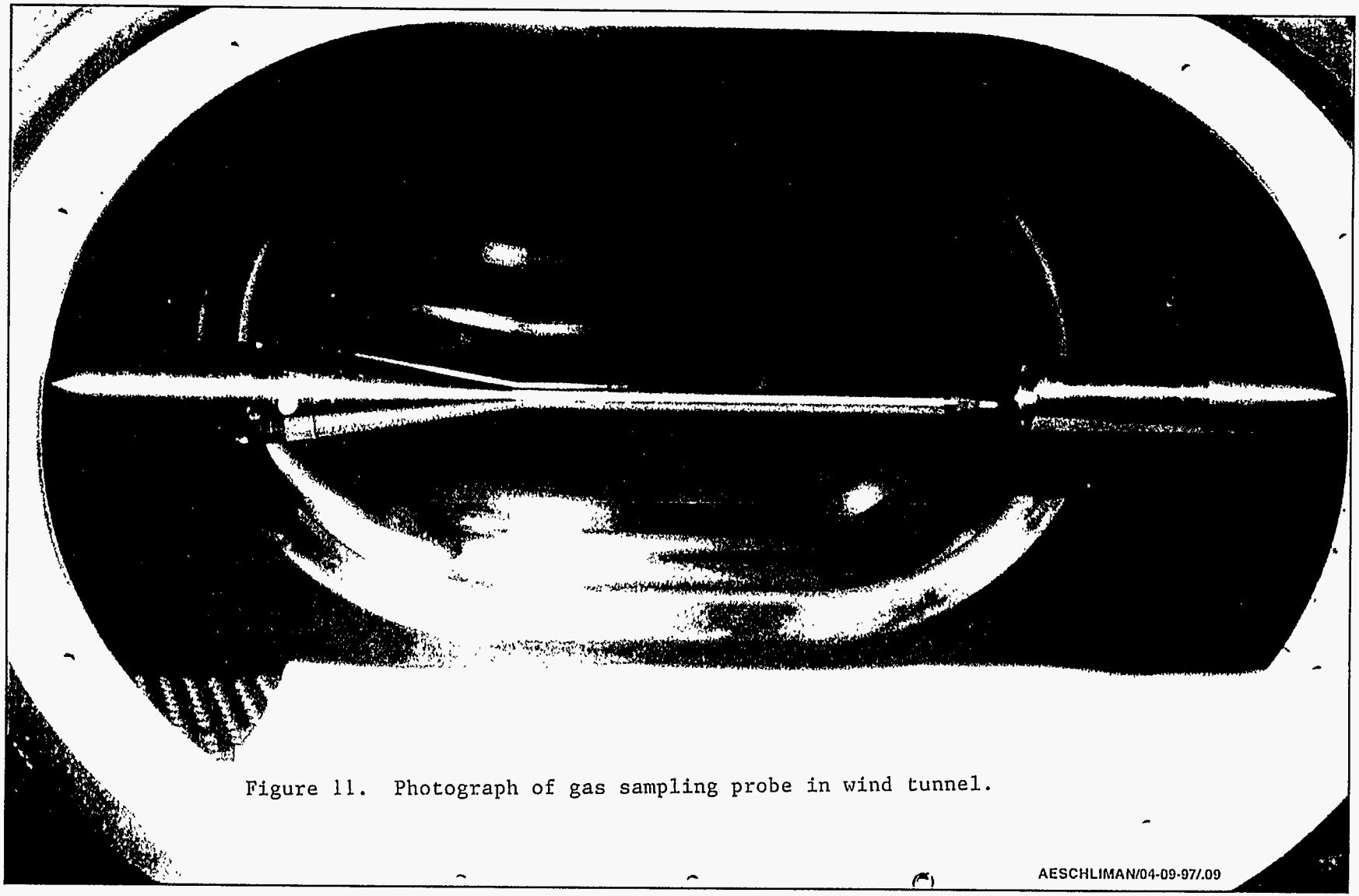

Figure 11. Photograph of gas sampling probe in wind tunnel.

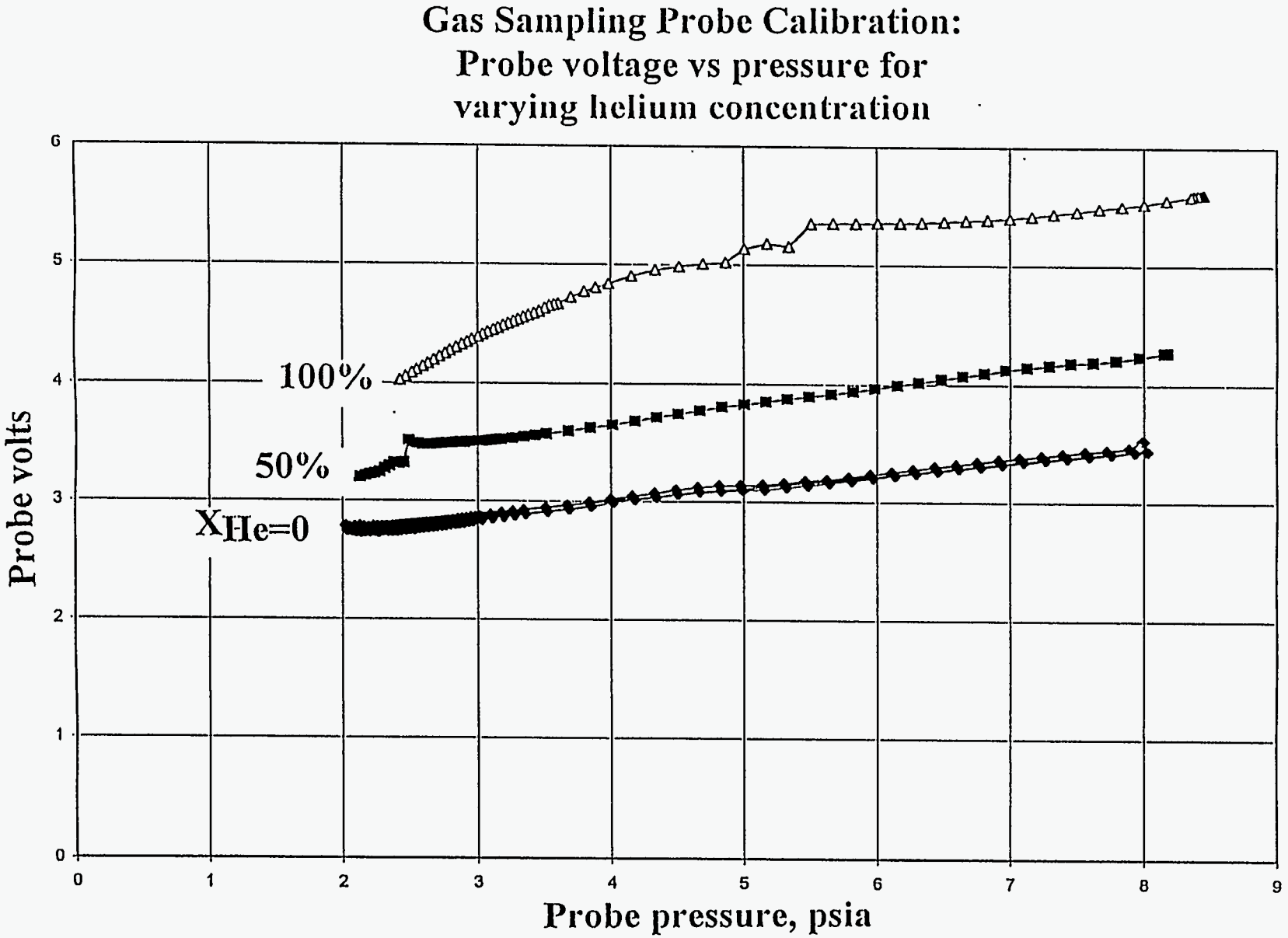

Figure 12. Representative calibration data for aspirating gas sampling probe, hot film voltage as a function of calibration tank pressure at 300K.

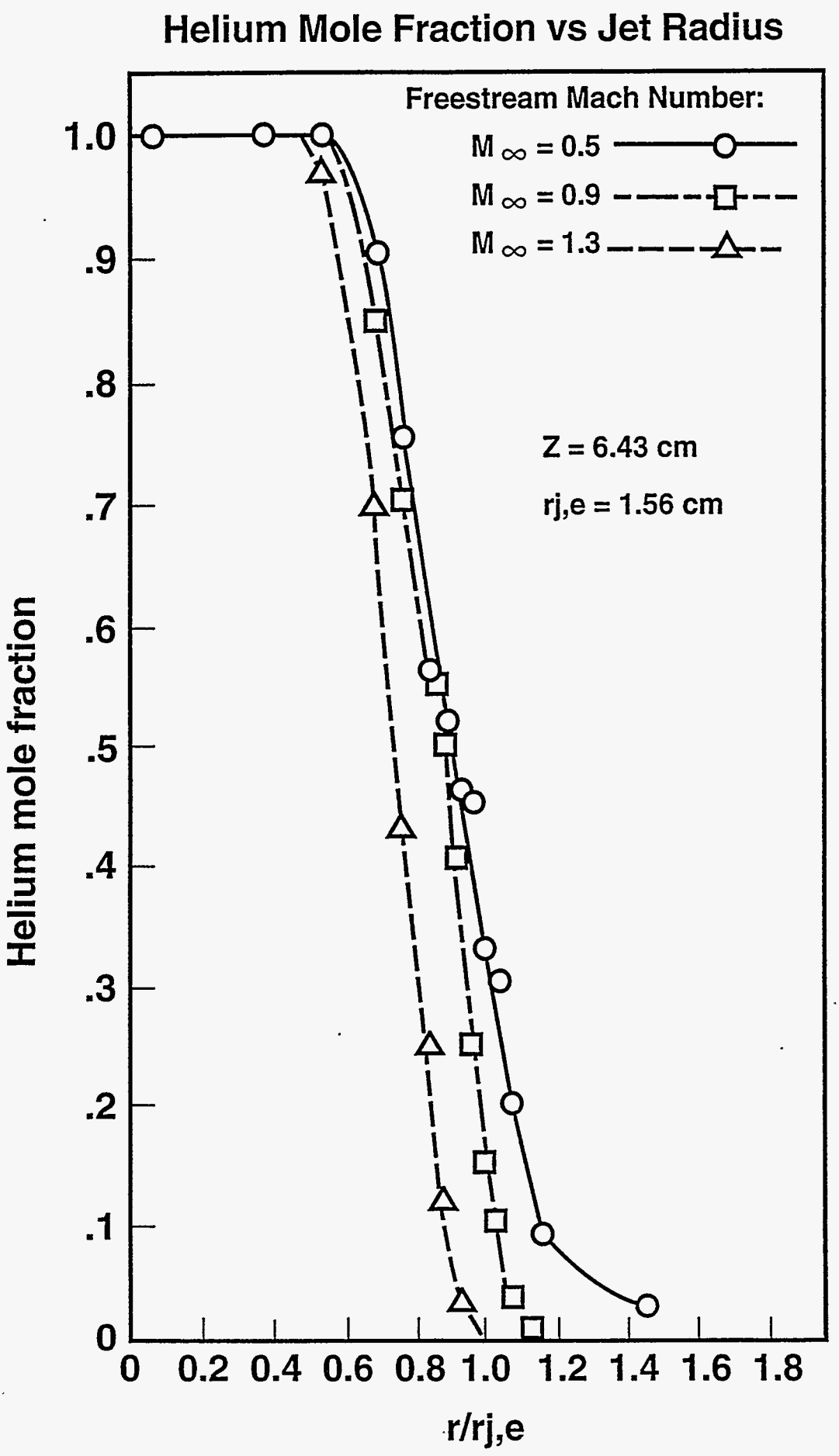

Figure 13. Helium mole fraction as a function of jet radius for subsonic helium jet in a coflowing air freestream of Mach number 0.5, 0.9, and 1.3.